

Experimental and Numerical Investigation into Turbulent High Reynolds Number Flows Through a Square Duct with 90-Degree Streamwise Curvature - II Numerical Methods

Dr. Faustin Ondore

Department of Aeronautical and Aviation Engineering
Technical University of Kenya
P.O. Box 52428-00200
Tel. +254724795469
Nairobi
Kenya

ABSTRACT

A square duct with a 90-degree streamwise curvature is representative of complex flow domains. Such flow domains are encountered in the designs of fluids engineering systems, especially in the aerospace turbo-machinery components. Examples include the gas turbine engine axial compressor inter-stage spaces, where the rise in air pressure (and hence compressor efficiency) is dependent on suppression of turbulence. In the case of the centrifugal compressor, pressure rise in the U-shaped diffuser assembly where the suppression of turbulence is critical to the attainable pressure ratio. The results obtained from numerical calculations are analysed and discussed along with the corresponding hot-wire measurements and flow visualization result from a wind-tunnel of identical configuration. Calculations are implemented in four turbulent models, i.e. Standard k- ϵ Module, Algebraic Stress Model (ASM), Non-linear Renormalization Group (RNG) - k- ϵ Model and Differential Stress Model (DSM). The discretization up-winding scheme is the Quadratic Up-winding with Interpolation Kinematics (QUICK). Two high Reynolds number turbulent flows are investigated, with mainstream velocities of 12.3 m/s and 20.4 m/s, representing $Re=3.56 \times 10^5$ and $Re=6.43 \times 10^5$ respectively. Generally strong correlation between theory and experimental data are recorded. Further, as reported in similar studies, the turbulence modules that are formulated to account for turbulence anisotropy return results that more closely match experimental measurements. Uniquely for this configuration, a massive flow detachment is predicted along the convex wall at about the 90° position. Also, the core of the fluid flow is observed to shift from the outer to the inner areas of the bend in proportion to the secondary (recirculating) flow generated by the bend.

1 INTRODUCTION

Highly turbulent flows investigated in this work pose difficult challenges, both experimentally and numerically. The overriding requirement is to resolve correctly and accurately the flow development prior to and well after exit of the bend. The primary numerical difficulty is the identification of a suitable turbulence model formulation. The second challenge is the availability of experimental data (produced or imported) that can be used for accurate capture of the essential physics of flow under study. In order to achieve credible physical results, complementary experimental data sets from this project were used. This approach has enabled closer analyses of flow parameters such as u , v , and k and ϵ in much greater detail. Very significantly, it was possible to predict a large flow bubble at the bend exit. This was also confirmed by smoke visualization. Details of the bent wind tunnel set up and measurements can be found in Ondore [1]. Other investigators have previously performed flow separation studies and reported very interesting results. Reference should be made to the works of Iacovides et al. [2] and, Luo and Lakshminarayana [3]. However, limited successes were reported in relation to flow separation. It is the author's view that such drawbacks originate with the deficiencies of imported data used in those calculations.

The square duct with streamwise 90-degree bend is shown in Figure 1 below.

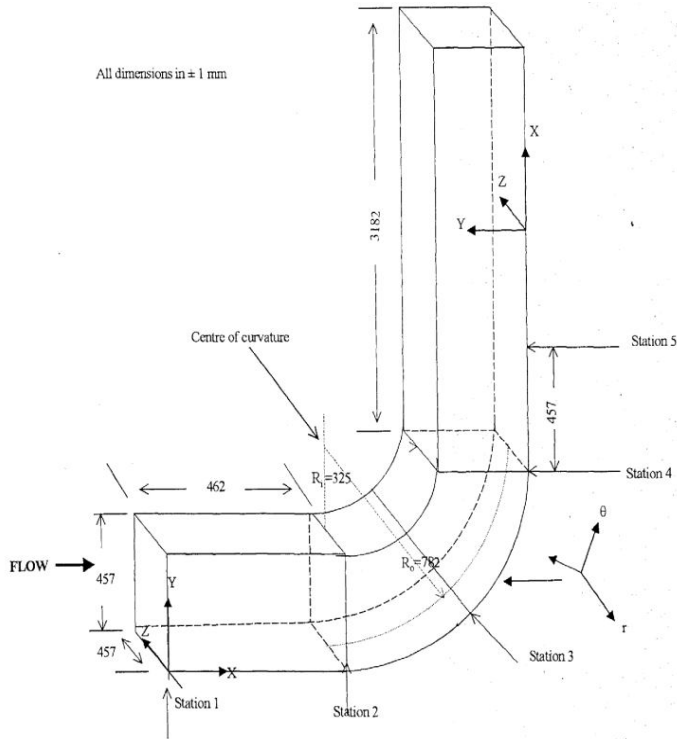


Figure 1: Square Duct With 90-Degree Bend

2 NOMENCLATURE

A duct cross-sectional area (457 x 457 mm)

C_p coefficient of pressure $\frac{p - p_{ref}}{\frac{1}{2} \rho u^2}$

D hydraulic duct diameter (457 mm) = $4A/4P$

k turbulent kinetic energy $\frac{1}{2} (\overline{u'^2} + \overline{v'^2} + \overline{w'^2})$

p duct section perimeter

p instantaneous pressure

p_{ref} reference pressure

\overline{p} mean pressure

r radial co-ordinate

R reference radius

R_c ratio of duct height to curvature

Re Reynolds number $\frac{U_\infty D}{\nu}$

R_i duct inner radius

R_o duct outer radius

R_m mean radius of curvature $\frac{R_o + R_i}{2}$

U_∞ mean free stream velocity

\overline{u} mean velocity in x-direction

u_p predicted u-velocity

u mean velocity in the x-direction

u' fluctuating velocity in x-direction

ν kinematic viscosity μ / ρ

ν_T eddy viscosity $\nu_T = C_\mu \frac{k^2}{\varepsilon}$

v mean velocity in the y-direction

v' fluctuating velocity in y-direction

$(\overline{u_{rms}^2} + \overline{v_{rms}^2})$ normal turbulence intensity

$\overline{u'v'}$ averaged cross product of u' and v'

V velocity vector $\sqrt{u^2 + v^2}$

x_D axial distance along duct tangent, expressed in hydraulic diameters

δ boundary layer thickness $0.99U_\infty$

δ_{ls} concave wall boundary layer thickness

δ_{us} convex wall boundary layer thickness

ε rate of dissipation of turbulence energy

κ von Karman's constant

μ molecular viscosity

μ_t turbulence viscosity

ν dynamic viscosity

τ_w wall shear stress

3 REVIEW OF PREVIOUS WORK

A number of turbulence models has been developed and used for the calculations of turbulent flows in complex geometries which are similar to the present bent duct. Square-sectioned domains with streamwise curvature are known to generate circular secondary flows which start from the corners of the duct. They also produce another kind of secondary flows that are perpendicular to the walls of the duct. Hence in order to simulate the flow successfully, the model formulation must capture not only the main characteristics of turbulence but also account for the anisotropy of the curvature-induced Reynolds stresses. Furthermore, the suppression of turbulence close the convex side must be predicted, as well as its enhancement in the concave wall regions. Numerical reproduction of these features of the flow is essential to the prediction of flow separation at the exit of the bend. Examples of turbulence model formulations which can be applied to calculation of curved flows are included in the works of Bradshaw [4], Hanjalic [5], Rodi and Scheurer [6], Launder [7], So et al. [8] and Speziale Thangam [9]. Details of turbulence models that are especially applicable to complex domains of the present geometry can be found in the studies of Irwin and Smith [10], Launder et al. [11], Hanjalic and Launder [12], Gibson [13], Gibson et al. [14], Gibson and Rodi [15], and Castro and Bradshaw [16]. A literature review was conducted to gain an understanding of the relative capabilities of various turbulence models in the calculation of such complex domain flows. Such comparative analyses can be found in the investigations of Choi et al. [17], Leschziner and Rodi [18], and Soritopoulos and Venticos [19]. Clearly, the superiority of the Differential Stress Model (DSM) in resolving secondary flows in square bent ducts is well established through these reviews. However, the DSM is found to be more costly in terms of computational resources, making the use of the more cost-effective Algebraic Stress Model (ASM) more appealing.

4 TURBULENCE MODELS

The main difficulty in this work is the accurate numerical capture of the full totality of the physics of highly turbulent developing flows in a square duct with 90-degree streamwise curvature. Partly for this reason, four different turbulence models were deployed. Because of its recognized superiority, the DSM which was originated by Launder et al. [11] offers the best prospects. Its mathematical formulations are detailed in the works of

Hanjalic and Launder [12], Gibson and Launder [20]. However, it is also recognized that the anisotropy of the Reynolds stresses can be more cost-effectively resolved by the (ASM). The details of the ASM can be found in Ljuboja and Rodi [21]. In this study, the more general approach advanced by Naot and Rodi [22], and Demuren and Rodi [23] is adopted. The third turbulence model used is the Renormalization Group Theory (RNG) $k-\epsilon$ Model developed by Yakhot and Orszag [24] and later used by Speziale and Thangam [9] in a study similar to the present configuration. Further information on the (RNG) $k-\epsilon$ Model formulation can be found in the works of Yakhot and Smith [25] and Yin et al. [26]. Turbulent shear stresses and the degree of anisotropy between the normal stresses are extremely sensitive to the effects of curvature. This sensitivity was particularly highlighted in a study conducted by Leschziner and Rodi [18]. In this regard the deficiencies of the Standard $k-\epsilon$ Model in the resolution of pressure-driven secondary flows of the present domain are well known and extensively documented, for example by Bradshaw [4], Launder et al. [11], Gibson and Rodi [15], and Luo and Lakhshminarayana [3]. However, it is included in this work mainly for the duo purposes of completeness and comparison.

The potential limitations of using imported data for theoretical calculations were fully recognized early in the project and decision made to incorporate parallel experimental airflow measurements as part of this project. Hence Hot-wire measurements were performed at duct planes of special interest (see Page 2, Figure 1). Thus, experimental data sets were used in the CFD calculations as well as in checking the correctness and accuracy of the numerical solutions. Wind-tunnel measurements and computational calculations were all performed at the Department of Mechanical Engineering at Brunel University, Uxbridge, England.

4.1 Governing Equations

Equations are solved for steady, incompressible and isothermal flows through the duct. Therefore within the straight tangents the differential equations are solved for continuity and momentum in the Cartesian coordinate system. In the bent section, differential equations are solved for continuity and momentum in cylindrical coordinate system. Full details of these equations can be found in Humphrey et al. [27]. The solution was obtained when the sum of all the cell residuals for each flow parameter normalized by the inlet mass flow reached a value of 0.5% or less.

5 DIFFERENCING SCHEME

In order to capture the nature and strength of secondary flows accurately, the Quadratic Upstream Interpolation of Convective Kinematics (QUICK) discretization scheme originated by Leonard [28] was employed in this work. It has been successfully used to solve convection–diffusion equations using second order central difference for the diffusion term. The scheme is third order accurate in space for the convection term, and first order accurate in time. The relative strengths of the QUICK formulation can be assessed by comparison to other differencing schemes, in relation to the resolution of longitudinal curvature effects on turbulent boundary layers, by reference to the investigations of Patel and Sotiropoulos [29], Han et al. [30] and Leschziner [31]. It was chosen in consideration for its accuracy and convergence performance.

6 NUMERICAL PROCEDURE

6.1 Grid

The physical duct domain was mapped onto the computational flow space by the use of curvilinear non-orthogonal co-ordinate transformation method originated by Thompson et al. [32]. In this method, the Cartesian coordinate system $(x) = (x, y, z)$ in the physical domain is replaced by $(\xi) = (\xi, \eta, \zeta)$ such that the boundaries corresponding with the surfaces $\xi = \text{constant}$. The grid is the multi-block type which consists of several blocks glued together in such a way that neighbouring cells meet in whole faces. In this way, no hanging nodes exist. Hence the computational duct space was divided into 176,000 cell with sizes geometrically adjusted to reflect flow conditions in the respective regions of the duct. The resultant grid structure is shown in Figure 2.

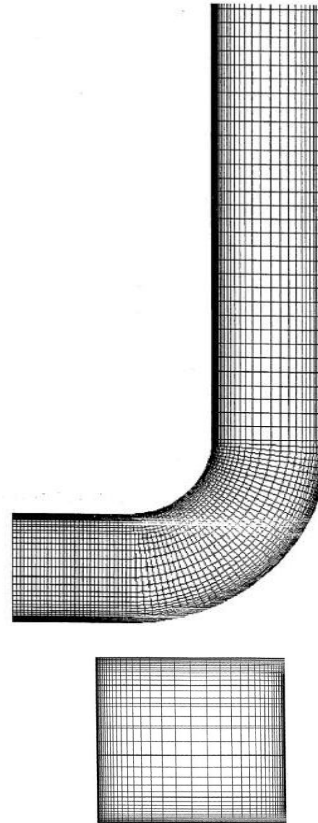


Figure 2: Streamwise and cross-duct grid distribution in duct

The velocity-pressure coupling algorithm adopted is the SIMPLEC (Semi-Implicit Method for Pressure Linked Equations-Consistent) formulation of Van Doormal and Raithby [33]. Details of the interpolation formulae employed to eliminate the oscillations associated with velocity-pressure coupling can be found in Rhie and Chow [34].

6.2 Boundary conditions

In order to capture the development state of the flows at the duct entry, measurements and calculations of velocities of the flows and values of k , ϵ , and Reynolds stresses were started upstream of the bend entry plane, at $x_D = -1.01$. The computations were started at this plane, using the measured data of flows incorporated via a FORTRAN sub-routine. Corresponding data from the exit plane were similarly inputted into the numerical code. The intensities of kinetic energy k are measured directly, but its dissipation rate ϵ is calculated from the proposal due to Choi et al. [15], i.e. $\epsilon = C^{3/4} k^{3/2} / \ell$, where the

length scale ℓ increases linearly with the normal distance from the wall, with the slope of 2.44 (reciprocal of the von Karman constant $\kappa = 0.4187$). Values of ε level off at approximately 0.5D.

Since the present study involves developing high Reynolds number flows with streamwise curvature, the resolution of the flows close to the walls is critical. In particular, it is noted that the boundary layers are only start to grow at the bend inlet. In contrast, where a fully turbulent flow is close to the wall, the y^+ value is selected such that $11.63 \leq y^+ \leq 500$. The first node must be sufficiently far from the wall such that the y^+ is greater than 11.63. Simultaneously, it must be close enough to the wall in order to resolve the flow features in the near wall region. An appropriate 'Wall Function' must be employed for the task. More details of 'wall function' methods can be found in Jones and Launder [35]. In the current case of developing turbulent flows the first node was placed typically at $30 \leq y^+ \leq 80$, according to the suggestions advanced by Humphrey et al. [27]. Further, the distance between the first nodal point P and the wall is bridged by a logarithmic velocity relation $u_p^+ = \frac{1}{\kappa} \ln(Ey_p^+)$,

$$u_p^+ = \frac{1}{\kappa} \ln(Ey_p^+),$$

$$\text{where, } u_p^+ = \frac{u_p}{(\tau_w/\rho)^{1/2}}, \quad y_p^+ = \frac{y_p(\tau_w/\rho)^{1/2}}{\nu} \text{ and}$$

$$E = 9.793.$$

$$\text{Equating the shear stresses, } \tau_p = \tau_w = \rho C_\mu^{1/2} k_p \quad \dots\dots\dots[1]$$

The turbulent kinetic energy can now be related to the shear stress at P through the equations for u_p^+ and τ_p :-

$$\tau_w = \frac{\rho \kappa C_\mu^{1/2} k_p^{1/2} u_p}{\ln\left(\frac{E y_p C_\mu^{1/4} k_p^{1/2}}{u}\right)} \text{ and } \varepsilon_p = \frac{C_\mu^{3/4} k_p^{3/2}}{\kappa y_p} \quad \dots\dots\dots[2]$$

Further details on the use of the technique can be found in Humphrey et al. [27].

6.3 Solution

The flows were determined to be highly turbulent and solved using the finite volume, Navier-Stokes Code CFX 4 (CFDS, AEA Technology, Harwell, UK) on non-orthogonal, body fitted grid employing the DSM, ASM, RNG-k- ε and Standard k- ε turbulent models. Grid independence tests were performed starting with a 100 x 30 x 30 initial grid, where the cell sizes were initially held constant in the normal coordinate direction whilst those in the streamwise coordinate direction were progressively reduced until no change could be discerned in the results. The procedure was then repeated with the streamwise coordinate cell sizes held constant whilst the sizes in the normal coordinate were reduced, again until no changes occurred in the results.

As indicated in Section 4.1, converged solution was obtained when the sum of all the cell residuals for each flow parameter normalized by the inlet mass flow reached a value of 0.5% or less.

7 RESULTS

7.1 Presentation

Figures 3 and 4 exhibit numerical results of mean velocities that are close to measured data, for $Re = 3.56 \times 10^5$ in the duct entry region.

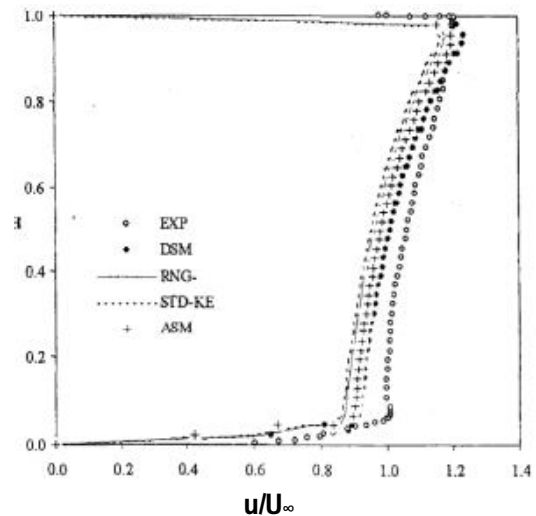


Figure 3: Station 2- $Re= 3.56 \times 10^5$

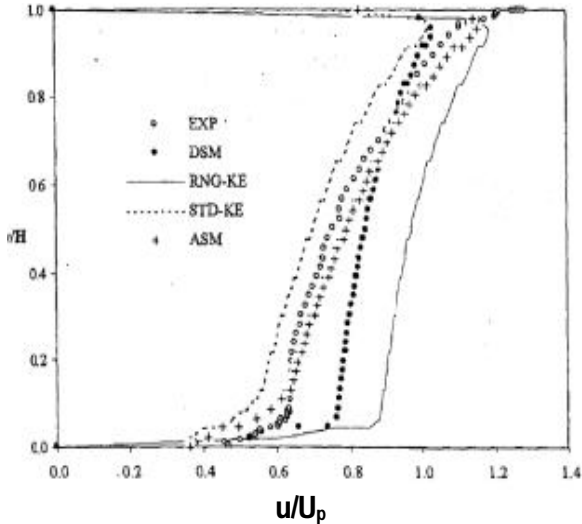


Figure 4: Station 3- $Re= 3.56 \times 10^5$

The skewed profiles of all the parametric plots provide the evidence of the bend influence well upstream of its entry plane. It clear from Figure 4 that substantial pressure gradient exists across the duct, causing the increase of turbulence intensity at the concave wall region. This also signifies the start of the shift of the core flow towards the convex side of the duct.

Strong secondary flow is simulated in Figure 5, especially at the duct corners where they are initiated by momentum deficiency, which is in turn generated cross stream by migration of fluid along the symmetry plane on one hand (convex to concave), and outer duct walls (concave to convex) on the other.

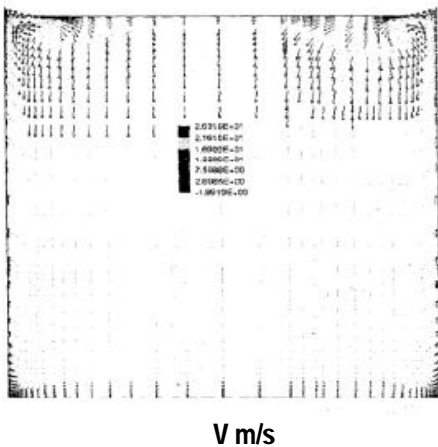


Figure 5: Station 4 - $Re= 3.56 \times 10^5$ corner secondary flows

Furthermore, the mechanism for turbulence suppression has resulted in greatly reduced shear stress intensity in the convex wall region (Figure 6).

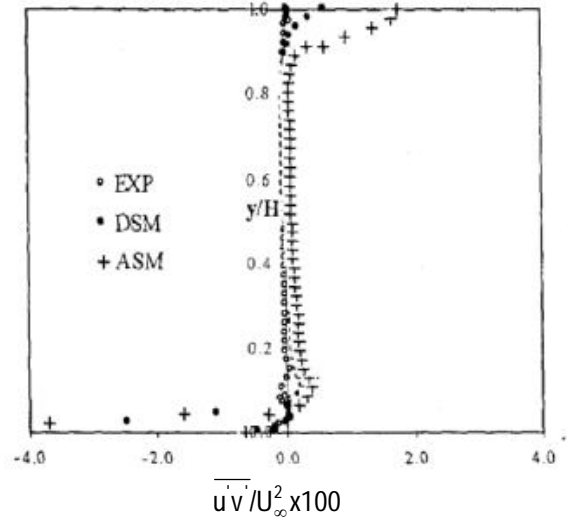


Figure 6: Station 4- $Re= 3.56 \times 10^5$

Figure 7 shows the start of recovery of the predicted velocity vector V_p along the concave wall from their minimum bend exit values. In contrast, the corresponding velocities assumed their maximum levels at the same location. The combined effects of these variations, in conjunction with resultant pressure gradients, have produced a large separation bubble depicted in Figure 8.

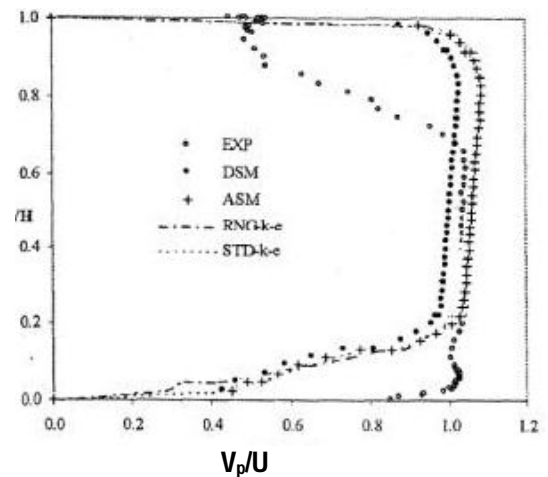


Figure 7: Station 5- $Re= 3.56 \times 10^5$

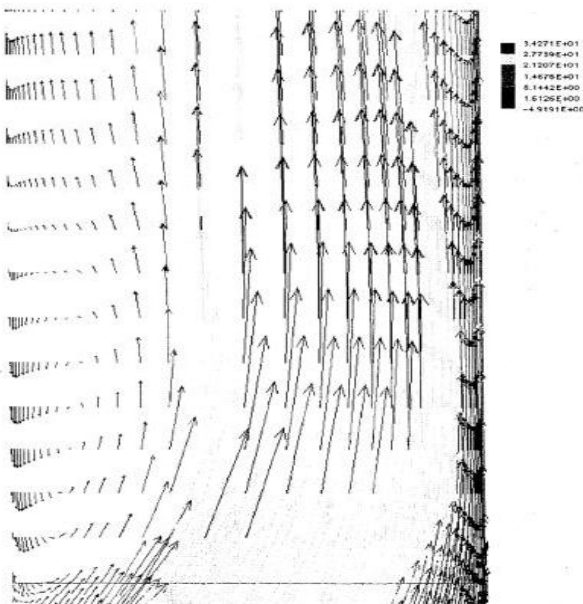


Figure 8: Station 5 - $Re = 6.43 \times 10^5$

Numerical prediction of flow separation was an interesting result that generated a fair amount of debate. It was decided to confirm this experimentally. Thus the experimental evidence is presented in Figure 9 below. To the author's knowledge no such separation in terms of scope and strength has been reported in the public domain in similar flow configuration.



Figure 9: Station 5 – Separation Bubble- $Re = 6.43 \times 10^5$

7.2 Discussion

The state of the boundary layer at the bend entry has a direct influence on the production of the secondary flow, turbulence intensities and movement of the inviscid fluid core between the pressure (concave) and suction (convex) wall. In addition, as elaborated elsewhere in this report, prediction of flow separation at the bend exit is only feasible with the correct resolution of the suppression of turbulence intensities at the suction wall. In turn, such correct resolution of the decrease in turbulence arguably depends almost entirely on the realism of the boundary conditions. As has already been pointed out, the use of correct empirical data in terms of both their qualitative and quantitative aspects was crucial to the result.

Although a favourable outcome was attained for the reasons stated earlier, it is important to consider the totality of the whole result. There are cases where numerical results showed significant differences with experimental data, which remained fairly consistent when compared to corresponding measurements from other sources. However, given the complexity of this type of domain and the fact the turbulence modeling is essentially an optimization process, this is perhaps not too surprising.

But the global aspect of the current solution appears to be in agreement with those of other workers. For example, the maximum shift of the core flows is observed at the 45-degree plane for both flows studied. A similar observation is made in the cases of the studies of Humphrey et al. [27] and Taylor et al. [36] where the shift was at the 77-degree location. But, in that case the Reynolds number was limited to 4×10^4 .

7.3 Conclusion

Experimental and numerical investigation of turbulent flows in complex geometries remains a challenging task. The experience from project is that both experiment and numerical modeling must be closely integrated if the best results are to be achieved. Furthermore, continuous improvements and hence further research in both spheres is essential. Given the critical importance of this type of investigation for development more efficient gas turbine engines for example, experimentalists and modelers must practice with greater all round collaboration.

ACKNOWLEDGMENTS

First, I wish to acknowledge the tremendous support and assistance availed by academic and other staff of the Department of Mechanical Engineering at Brunel University. Special thanks are due to my PhD supervisor, Prof. Reza Mokhtarzadeh-Deghan. Further, it is important to accept the extremely useful comments and suggestions received from many individuals during the ASME FED conferences where aspects of this work were discussed. Lastly, I am very grateful to the comments of the reviewers, without whose input this work would not have reached its current status.

REFERENCE

- [1] Ondore, F. A., 2003, "Experimental and Numerical Investigation of Turbulent High Reynolds Number Flows in a Square Duct With 90-Degree Streamwise Curvature: Part 1 — Experiment" ASME/JSME 2003 4th Joint Fluids Summer Engineering Conference Paper No. FEDSM2003-45585, pp. 1077-1093.
- [2] Iacovides, H., Launder B.E., and Loizou, P.A., 1987, "Numerical Computation of Turbulent Flow Through a Square-sectioned 90-Degree Bend", ASME Journal of Heat and Fluid Flow, 8, (4), pp. 320-325.
- [3] Luo, J., and Lakshminarayana, B., 1997, "Prediction of Strongly Curved Turbulent Duct Flows With Reynolds Stress Model", Journal of American Institute of Aeronautics and Astronautics, 35, pp. 91- 98.
- [4] Bradshaw, P., 1973, "Effects of Streamline Curvature on Turbulent Flows" North Atlantic Treaty Organisation, AGARDograph, 169, pp. 1-72.
- [5] Hanjalic, K. 1994, "Advanced Turbulence Closure Models: A Review of Current Status and Future Prospects," International Journal of Heat and Fluid Flow, 15, (3), pp. 458 – 463.
- [6] Rodi, W., and Scheuerer, G., 1983, "Calculation of Curved Shear Layers with Non-Linear Two-Equation Models" Journal of Fluids of Physics, 26, (6), pp. 1422 – 1435.
- [7] Launder, B. E., 1990 "Whither turbulence? Turbulence at cross roads" Lecture Notes in Physics, 537, pp. 439 – 485, Springer, Berlin.
- [8] So, R. M. C., Lai, Y. G., and Hwang, B. C., 1991, "Secondary order near-wall turbulence closure" J. AIAA, 29, (11), pp. 1202 – 13.
- [9] Speziale, G. C., and Thangam, S. 1992 "Analysis of RNG-based Turbulence Model for Separated Flows" International Journal of Engineering Science, 30, (10), pp. 1379 – 1388.
- [10] Irwin, H. P. A. H., and Smith, P. A., 1975, "Prediction of the Effect of Curvature on Turbulence" The Physics of Fluids, 18, (6), pp. 624 – 630.
- [11] Launder, B. E., Reece G. J., and Rodi, W., 1975 "Progress in the Development of a Reynolds-Stress Turbulence Closure", Journal of Fluid Mechanics, 68, (3), pp. 537 – 566.
- [12] Hanjalic, K and Launder, B. E. 1972 "A Reynolds-stress Model of Turbulence and its Application to Thin Shear Thin Layers," Journal of Fluid Mechanics, 52, pp. 609 – 638.
- [13] Gibson, M.M., 1978, "An Algebraic Stress and Heat-Flux Model for Turbulent Shear Flows with Streamline Curvature" Int. Journal of Mass and Heat Transfer", 21, pp. 1609 – 1617.
- [14] Gibson, M.M., Jones, W.P., and Younis, B. A. 1981, "Calculation of Turbulent Boundary Layers On Curved Surfaces" Journal of Physics of Fluids, 24(3), pp. 386 – 395.
- [15] Gibson, M.M., and Rodi, W., 1981, "A Reynolds-Stress Closure Model of Turbulence Applied to the Calculation of a Highly Curved Mixing Layer," Journal of Fluid Mechanics, 103, pp. 161 – 182.
- [16] Castro, I., and Bradshaw, P., 1976, "The Structure of a Highly Curved Mixing Layer" Journal of Fluid Mechanics, 73, pp. 265 – 304.
- [17] Choi, Y.D., Iacovides, H., and Launder, B. E., 1989 "Numerical Computation of Turbulent Flow in a Square-Section 180-Degree Bend" ASME: Journal of Fluids Engineering, 111, Pp. 59 – 66.
- [18] Leschziner, M. A., and Rodi, W., 1981, "Calculation of Annular and Twin Parallel Jets Using Various Differencing Schemes and Turbulence Model Variations", ASME Journal of Fluids Engineering, 103, pp. 352-360.
- [19] Soritopoulos, F., and Venticos, Y., 1998, "Flow Through a Curved Duct Using Non-Linear Two-Equation Models", AIAA Journal, 36, (7), pp. 1256 – 1262.
- [20] Gibson, M. M., and Launder, B. E. 1978, "Ground Effects on Pressure Fluctuations in the Atmospheric Boundary Layer," Journal of Fluid Mechanics, 86, pp. 491-511.
- [21] Ljuboja, M., and Rodi, W. [1980], "Calculation of Wall Jets With an Algebraic Stress Model", ASME Journal of Fluids Engineering, 102 (3), pp. 350-356.
- [22] Naot, D., and Rodi, W., 1982, "Numerical Simulation of Secondary Currents in Channel Flows", Journal of American Society of Civil Engineers, 108 (HY8), pp. 948-968.

- [23] Damuren, A. O., and Rodi, W., 1984, "Calculation of Turbulence Driven Secondary Motion in Non-Circular Ducts", *Journal of Fluid Mechanics*, 140, pp. 189-222.
- [24] Yakhot, V., and Orszag, S.A., 1986, "Renormalization Group Analysis of Turbulence: 1. Basic Theory" *Journal of Scientific Computation*1(l), (Part 3).
- [25] Yakhot, V. and Smith, L. M., 1992 "The Renormalization group, the ϵ -expansion and derivation of turbulence models", *Journal of Scientific Computing*, (7), No. 1.
- [26] Yin, M., Shi, F. and XU, Z., 1996, "Renormalization group theory based k- ϵ turbulence model for flows in a duct with strong curvature", *International Journal of Engineering Science*, 34 (2) pp. 243 – 248.
- [27] Humphrey, J. A. C., Whitelaw, J. H. and Yee, G. 1981, "Turbulent flow in a square duct with strong curvature" *Journal of Fluid Mechanics*, 103, pp. 443 – 463.
- [28] Leonard, B. P., 1979", A Stable and Accurate Convective Modeling Procedure Based on Quadratic Upstream Interpolation", *Computer Methods in Applied Mathematics and Engineering*, 19, pp. 59-98.
- [29] Patel, V.C., and Sotiropoulos, F., 1996, "Longitudinal Curved Effects in Turbulent Boundary Layers", *Progress in Aerospace Science*, 33, pp. 1-70.
- [30] Han, T., Humphrey, J. A.C., and Launder, B. E. 1981, "A Comparison of Hybrid and Quadratic Upstream Differencing in High Reynolds Number Elliptic Flows," *Computer Methods in Applied Mechanics and Engineering*, 29, pp. 81 – 95.
- [31] Leschziner M. A., 1980, "Practical Evaluation of Three Differencing Schemes for the Computation of Steady State Re-circulating Flows", *Journal of Fluids Engineering*, 23, pp. 352 – 360.
- [32] Thompson, J. F., Warsi Z. U.A., Mastin C. W. 1985, "Numerical Grid Generation: Foundations and Applications" North-Holland.
- [33] Van Doormal, J. P. and Raithby, G. D. 1984, "Enhancement of SIMPLE method for Predicting Incompressible Fluid Flows" *Numerical Heat Transfer*, 7, pp. 147-163.
- [34] Rhie, C. M. and Chow, W. L. 1983, "Numerical Study of Turbulent Flow Past an Aerofoil With Trailing Edge Separation" *AIAA Journal*, 21 (1), pp. 1527 – 1532.
- [35] Jones, W. P. and Launder, B. E. 1972, "The Prediction of Laminarization With a Two-Equation Turbulence Model" *International Journal of Heat & Mass Transfer*, 15, pp. 301-314.
- [36] Taylor, A., Whitelaw, J. and Yianneskis, M. 1982, "Curved Ducts With Strong Secondary Flow: Velocity Measurements of Developing Laminar and Turbulent Flow" *ASME Journal of Fluids Engineering*, 104, pp. 350-354.